

## Quasi-chemical Phase Diagrams for Orienting Mixtures

Yuri Hueda and María Eugenia Costas

Facultad de Química, Universidad Nacional Autónoma de México, México 04510, D.F., México

Robert L. Scott\*

Department of Chemistry and Biochemistry, University of California, Los Angeles, California 90095

Received: March 31, 1997<sup>®</sup>

Phase diagrams of quasi-lattice mixtures with orienting forces are calculated using the quasi-chemical approximation. Two different coordination numbers and three different cases of the interaction parameters between faces of molecules are studied. In some, closed loops are observed, while in others extra features like several different three-phase regions, triple points, double critical points, and a special point, a critical double point, are found.

### Introduction

A wide variety of binary mixtures show regions of coexistence between two liquid phases. This immiscibility usually decreases as the temperature is raised, and disappears above an upper critical solution temperature (UCST) unless vaporization occurs first. In a few mixtures, however, the extent of the liquid–liquid coexistence region decreases as the temperature is lowered and the mixture becomes completely miscible again at temperatures below another (lower) critical solution temperature (LCST). This sequence of phase transitions from an LCST to a UCST is known as a closed-loop phase diagram.

For many years this phenomenon has been explained, at least qualitatively, in terms of the balance between entropy and energy effects at different temperatures. Suppose that molecules exhibit van der Waals interactions and short-range attractions highly dependent on a specific orientation, such as hydrogen bonding, occur between unlike molecules. Suppose further that, for all other orientations of unlike pairs, the attraction is weaker than those between like pairs. The high directionality of the specific interaction implies that there is a lower number of possible configurations, and so this interaction is entropically disfavored. At sufficiently high temperatures the differences between the various interactions are relatively unimportant and a more or less randomly distributed homogeneous mixture is found since this situation is entropically favored. As temperature decreases, the stronger van der Waals attractions between like molecules dominate, and the system segregates into two coexisting phases. At still lower temperatures, however, the entropic disadvantage of any special orientation is overcome, and the system becomes miscible again favoring the strong oriented interactions between unlike molecules. This means that the balance between the different kinds of interactions in the mixture can produce both an upper and a lower critical temperature.

The statistical thermodynamics of liquid mixtures with orienting forces has been a subject of interest for many years. Early classical theoretical approaches include those that use a simple lattice model,<sup>1–3</sup> mainly based upon the quasi-chemical equations of Guggenheim,<sup>4</sup> and those that are extensions of a corresponding states treatment of solutions.<sup>5,6</sup> These early papers were concerned with thermodynamic functions and vapor pressures, and, with the exception of one paper by Barker and Fock,<sup>7</sup> none considered phase equilibria. After a decade or more

in which the subject lay dormant, new theoretical approaches have been developed for calculating phase diagrams of this type of mixture: decorated lattice models,<sup>8,9</sup> renormalization group calculations,<sup>10</sup> numerical simulations,<sup>11</sup> models based upon chemical equilibrium,<sup>12,14</sup> and analytic equations extending that of van der Waals.<sup>13</sup> All of these get closed loops, but only a few get additional features.

Of the above models, the quasi-chemical approximation was not used extensively to predict the phase diagrams of multi-component systems, mainly due to the complexity of the equations involved in the calculation of the thermodynamic states. Nevertheless, with the use of fast computers, the solution of the model's equations has become much easier. In this paper we report calculations of phase diagrams for three different sets of energy–parameter relations using the quasi-chemical approximation. We find a richer behavior than that reported by Barker and Fock<sup>7</sup> using essentially the same model.

### The Model

Our model follows those of Barker<sup>2</sup> and Tompa<sup>3</sup> with some generalization of the specific model of Barker and Fock.<sup>7</sup> The molecules  $N_\alpha$  of species  $\alpha$ ,  $N_\beta$  of species  $\beta$ , etc., are distributed on a quasi-lattice of coordination number  $z$ , each molecule occupying one lattice site. Let each molecule be capable of  $z'$  discrete orientations, each labeled 1, 2, ...,  $i$ , ...,  $z'$ . (It will be convenient to regard  $z = z'$ , but this is not necessarily the case even in a rigid lattice; for example, in the face-centered cubic lattice,  $z = 12$ , but there can be  $z' = 24$  distinct orientations. Any kind of symmetry in the molecule, however, reduces  $z'$  to  $z$  or smaller.)

We consider only nearest-neighbor interactions and designate the energy of a pair of nearest-neighbor molecules  $\alpha\beta$  in orientations  $p$  and  $q$ , respectively, as  $\epsilon_{\alpha\beta}^{pq}$  and the number of such pairs as  $N_{\alpha\beta}^{pq}$ . Assuming  $z = z'$ , there are thus  $z^2$  kinds of mutual orientation for each  $\alpha\beta$  pair. (Alternatively, one may regard the  $z^2$  different interactions as arising from the contact between different faces of the molecules. There is, of course, a physical difference between two such models, and the assignment of parameters will differ between, say, a model of interactions between orientations of point dipoles or point quadrupoles [Tompa], and a model of surface contacts [Barker]; however, the formal mathematics is identical.)

<sup>®</sup> Abstract published in *Advance ACS Abstracts*, October 1, 1997.

The number of nearest-neighbors pairs  $N_{\alpha\beta}^{pq}$  can be written as

$$N_{\alpha\beta}^{pq} = Nx_{\alpha}x_{\beta}(1 + \xi_{\alpha\beta})/(2z) \quad (1)$$

where  $N$  is the total numbers of molecules in the system,  $x$  is mole fraction, and  $\xi$  is a deviation parameter; where the distribution of pairs entirely random, all the  $\xi$ 's would be zero.<sup>15</sup> The configurational free energy can then be written as

$$\frac{A_{\text{conf}}}{NkT} = \sum_{\alpha} x_{\alpha} \ln x_{\alpha} + \left(\frac{1}{2z}\right) \sum_{\alpha} \sum_{\beta} x_{\alpha} x_{\beta} \sum_p \sum_q (1 + \xi_{\alpha\beta}^{pq}) \left[ \ln(1 + \xi_{\alpha\beta}^{pq}) + \frac{\epsilon_{\alpha\beta}^{pq}}{kT} \right] \quad (2)$$

where, as usual,  $k$  is the Boltzmann constant and  $T$  is the thermodynamic temperature. From eq 2 the familiar quasi-chemical equation can be derived and expressed in the following simple form:

$$\ln \frac{(1 + \xi_{\alpha\beta}^{pq})^2}{(1 + \xi_{\alpha\alpha}^{pp})(1 + \xi_{\beta\beta}^{qq})} = \ln K_{\alpha\beta}^{pq} = -2 \frac{\epsilon_{\alpha\beta}^{pq} - \epsilon_{\alpha\alpha}^{pp} - \epsilon_{\beta\beta}^{qq}}{kT} = -2 \frac{\epsilon_{\alpha\beta}^{pq}}{kT} \quad (3)$$

where on the extreme right-hand side we have, with no loss in generality, chosen a zero of energy by setting  $\epsilon_{\alpha\alpha}^{pp}$  and  $\epsilon_{\beta\beta}^{qq}$  equal to zero. Note that the equilibrium constants  $K_{\alpha\beta}^{pq}$  do not include an entropy factor 4; for the ideal case they all reduce to unity. For the configurational Helmholtz free energy, after some simplification, we have

$$\frac{A_{\text{conf}}}{NkT} = \sum_{\alpha} x_{\alpha} \left[ \ln x_{\alpha} + \left(\frac{1}{2}\right) \sum_p \ln(1 + \xi_{\alpha\alpha}^{pp}) \right] \quad (4)$$

There is a conservation condition for each face (or orientation)  $p_{\alpha}$  which can be written in the general form

$$(1 + \xi_{\alpha\alpha}^{pp})^{1/2} \sum_{\alpha} x_{\alpha} \sum_q [K_{\alpha\beta}^{pq} (1 + \xi_{\beta\beta}^{qq})]^{1/2} = z \quad (5)$$

Note that the summation over  $q$  includes all orientations including  $p$ . It is eqs 3, 4, and 5 that the earlier workers,<sup>2,3,7</sup> working without modern computers, solved so painfully for special cases more than 40 years ago.

Using this formulation, we calculated several cases in which the interaction parameters are assigned to pairs of nearest-neighbor faces of the molecules. We considered a binary mixture of A and B species, the A molecules with  $z - 1$  faces of types  $a$  and one of type  $x$ , and the B molecules with  $z - 1$  faces of type  $b$  and one of type  $y$ . Although there are in principle 10 different energy parameters, we have reduced them to four by taking  $\epsilon_{aa}$ ,  $\epsilon_{xx}$ ,  $\epsilon_{ax}$ ,  $\epsilon_{bb}$ ,  $\epsilon_{yy}$ , and  $\epsilon_{by}$  equal to zero. (It should be noted that our model thus assumes no orientation in the pure components; this makes  $A_{\text{conf}}$  equal to the free energy of mixing  $\Delta A$ .) Because of these choices, the four remaining parameters can be effectively attractive or repulsive depending on the type of mixture we are analyzing. For this model, the

four conservation relations (5) are

$$(1 + \xi_{aa})^{1/2} \{ (1 - x)[(z - 1)(1 + \xi_{aa})^{1/2} + (1 + \xi_{xx})^{1/2}] + x[(z - 1)K_{ab}^{1/2}(1 + \xi_{bb})^{1/2} + K_{ay}^{1/2}(1 + \xi_{yy})^{1/2}] \} = z$$

$$(1 + \xi_{xx})^{1/2} \{ (1 - x)[(z - 1)(1 + \xi_{aa})^{1/2} + (1 + \xi_{xx})^{1/2}] + x[(z - 1)K_{bx}^{1/2}(1 + \xi_{bb})^{1/2} + K_{xy}^{1/2}(1 + \xi_{yy})^{1/2}] \} = z$$

$$(1 + \xi_{bb})^{1/2} \{ (1 - x)[(z - 1)K_{ab}^{1/2}(1 + \xi_{aa})^{1/2} + K_{xy}^{1/2}(1 + \xi_{xx})^{1/2}] + x[(z - 1)(1 + \xi_{bb})^{1/2} + (1 + \xi_{yy})^{1/2}] \} = z$$

$$(1 + \xi_{yy})^{1/2} \{ (1 - x)[(z - 1)K_{ay}^{1/2}(1 + \xi_{aa})^{1/2} + K_{xy}^{1/2}(1 + \xi_{xx})^{1/2}] + x[(z - 1)(1 + \xi_{bb})^{1/2} + (1 + \xi_{yy})^{1/2}] \} = z \quad (6)$$

where  $x$  is the mole fraction of B (sites  $b$  and  $y$ ). From these conservation conditions, given values of the  $K$ 's, one can calculate for various values of  $x$  the four deviation parameters and their first and second derivatives. With these one can then calculate the Helmholtz free energy  $A$  and its derivatives as functions of  $x$ , from which all the necessary phase diagrams can be determined. We use the following two parameters to illustrate the various kinds of phase diagrams:

$$r = -\frac{\epsilon_{xy}}{\epsilon_{ab}} = -\frac{\ln K_{xy}}{\ln K_{ab}}; \quad \theta = \frac{kT}{2\epsilon_{ab}} = -\frac{1}{\ln K_{ab}} \quad (7)$$

We characterize the different mixtures by the  $r$  parameter and show the behavior in the phase diagrams with the reduced temperature  $\theta$ .

## Results

We calculated the phase diagrams for this model by setting the values of the parameters  $r$  and  $\theta$ , which in turn determine the  $K_{ab}$  and  $K_{xy}$  values. We set  $K_{ab} < 1$ , taking the energy of the  $ab$  pair as repulsive, and  $K_{xy} > 1$ , taking the energy of the  $xy$  pair as attractive; in this way  $r$  and  $\theta$  are always positive. We distinguish three cases, depending upon the nature of the  $ay$  and  $bx$  interactions. Calculations were made for mixtures with two different values of the coordination number  $z = 4$  and  $z = 6$ :

case I:

$$\epsilon_{ab} > 0 \rightarrow K_{ab} < 1$$

$$\epsilon_{ay} = \epsilon_{bx} = \epsilon_{xy} < 0 \rightarrow K_{ay} = K_{bx} = K_{xy} > 1$$

$$\epsilon_{ax} = \epsilon_{by} = 0 \rightarrow K_{ax} = K_{by} = 1$$

$\theta$ - $r$  diagrams for case I,  $z = 4$  and  $z = 6$ , are shown in Figure 1; the lines represent critical points, at which the second derivative of the free energy is equal to zero. We calculated the free energy as a function of composition for a fixed  $r$  at different  $\theta$  values, and we found that for each  $r$  value two critical points at different  $\theta$  are observed, both at  $x = 1/2$ . In Figure 2 we show the phase diagrams for  $z = 4$  and  $z = 6$  at different  $r$  values; in both cases closed loops are observed. As can be seen in this figure, for  $z = 6$  the range of temperature over which a closed loop is observed is larger than for  $z = 4$ . The reason for this is that for  $z = 6$  there are a larger number of repulsive pairs  $N_{ab}$  that produce phase separation over a wider temperature

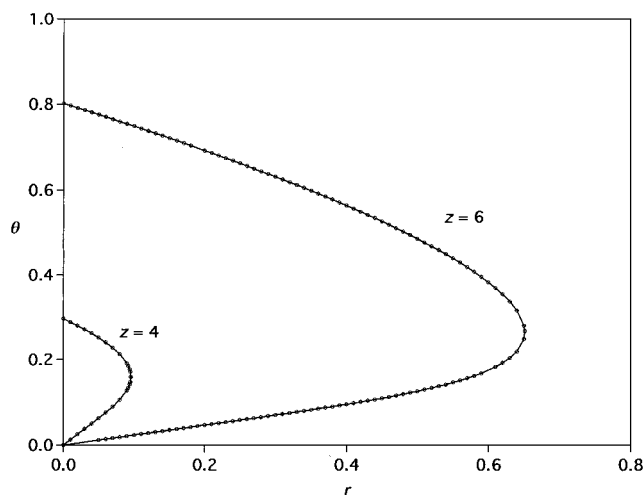


**Figure 1.**  $\theta$ - $r$  master diagrams for case I with  $z = 4$  and  $z = 6$ . Symmetrical critical points,  $\bigcirc$ - $\bigcirc$ .

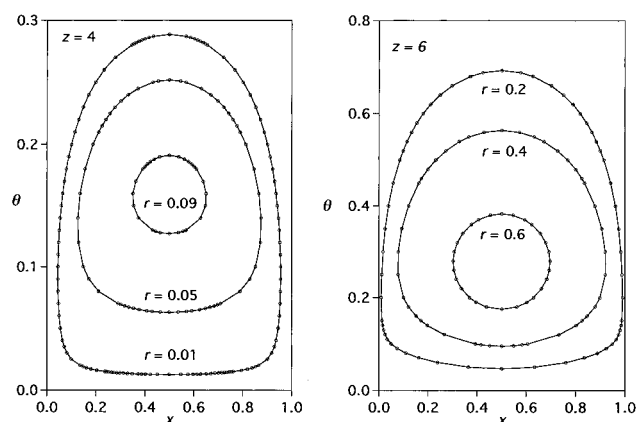


**Figure 2.** Closed-loop  $\theta$ - $x$  diagrams for case I,  $z = 4$  and  $z = 6$ , for various  $r$ 's.

range. For  $r > 0.0955$  ( $z = 4$ ) and  $r > 0.6512$  ( $z = 6$ ) the system is homogeneous at all temperatures.

case II:

$$\epsilon_{ab} > 0 \rightarrow K_{ab} < 1$$

$$\epsilon_{xy} < 0 \rightarrow K_{xy} > 1$$

$$\epsilon_{ax} = \epsilon_{by} = \epsilon_{ay} = \epsilon_{bx} = 0 \rightarrow K_{ax} = K_{by} = K_{ay} = K_{bx} = 1$$

For case II and  $z = 4$ , the same qualitative features as case I are observed. On the contrary, for case II and  $z = 6$  new features are found in the  $\theta$ - $r$  master diagram (Figure 3). We calculated the free energy as a function of composition for selected  $r$  values and found that these systems can show a wide variety of phase behavior: a triple line, a double critical line, and a special point, namely a critical double point. There is a line (dotted) that does not represent ordinary critical points, although it is a line where the second derivative of the free energy is equal to zero: it is a point where a metastable phase (at  $x = 0.5$ ) becomes unstable; thus it is a special kind of spinodal line.

Figure 4 shows a progression of phase diagrams as a function of  $r$ . For none of these does one find a simple liquid-liquid phase diagram with a single upper critical end point. For all of them there are, at sufficiently low temperatures, two two-phase regions separated by a one-phase region around  $x = 0.5$ . For all  $r$  between 0 and 2.214 83 these separate two-phase regions persist up to a triple-point temperature above which there

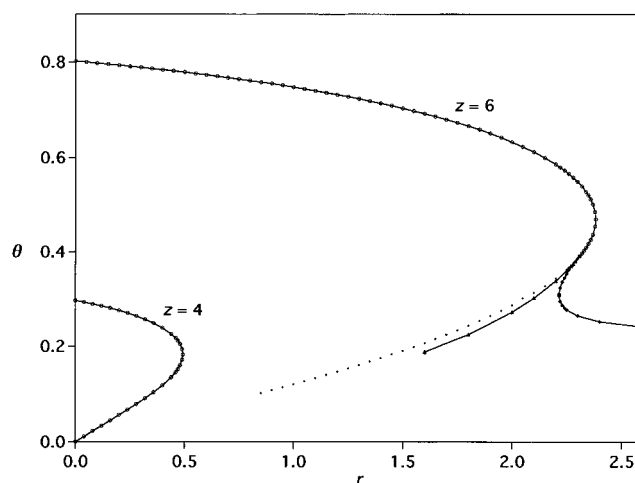


**Figure 3.**  $\theta$ - $r$  master diagrams for case II with  $z = 4$  and  $z = 6$ . Symmetrical critical points,  $\bigcirc$ - $\bigcirc$ ; unsymmetrical critical points,  $\blacklozenge$ - $\blacklozenge$ ; triple points,  $\blacktriangle$ - $\blacktriangle$ ; metastable critical points,  $\bullet$ .

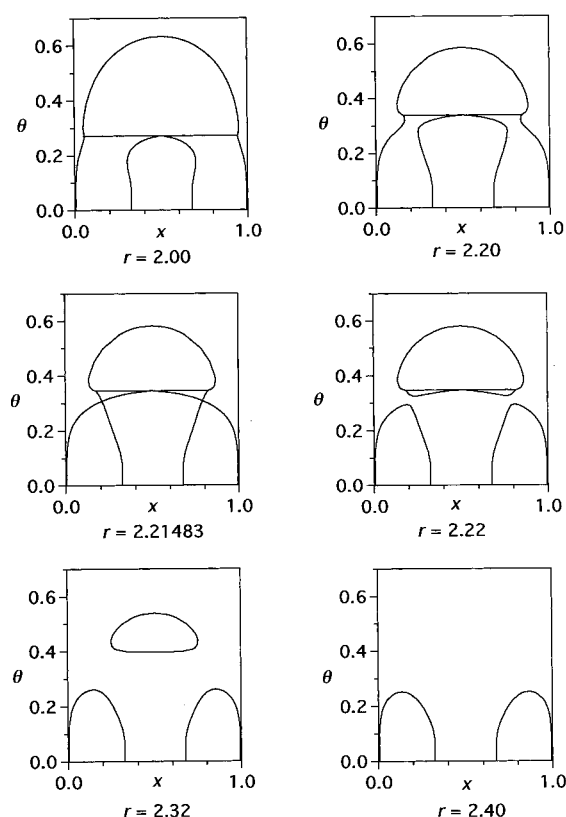


**Figure 4.**  $\theta$ - $x$  phase diagrams for case II,  $z = 6$ , for various  $r$ 's, showing complex diagrams.

is a single symmetrical two-phase region that ends with an upper critical solution point at  $x = 0.5$ . (For the special case  $r = 0$ , as seen in Figure 3, the triple point is at  $\theta = 0$ .) At  $r = 2.214\ 83$  and  $\theta = 0.308\ 15$ , there is a pair of critical double points. For a range of  $r$  values above 2.214 83, there are five distinct two-phase regions, each with a critical solution point.

Between  $r = 2.312$  and  $2.313$  (the exact calculation is difficult) the triple-point line merges with the critical point line (see Figure 3); that is, the three triple-point compositions have merged at  $x = 0.5$ . For a while three two-phase regions persist, but finally, at  $r = 2.3828$ , the high-temperature closed loop has shrunk to a double critical point, and above this value only the two distinct low-temperature two-phase regions remain. It can be shown, at least for this model, that these regions persist to zero temperature, where the length of the tie-line is

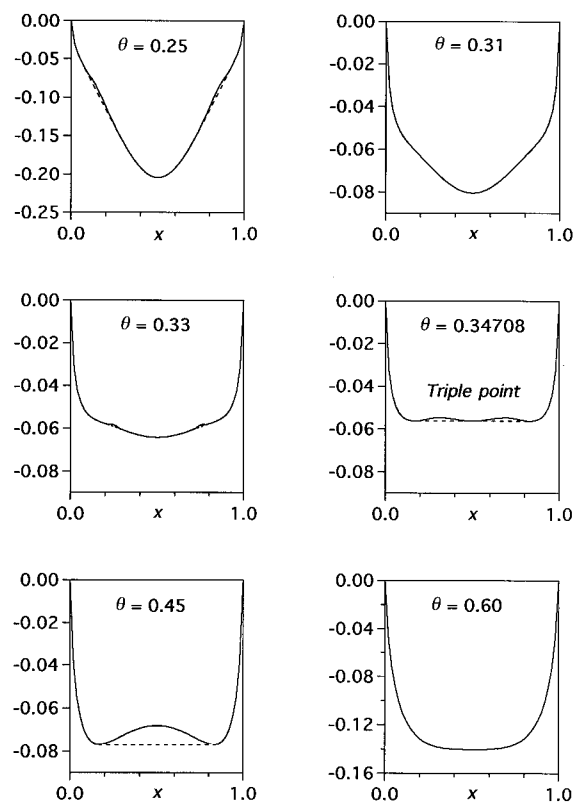


**Figure 5.** Free energy diagrams [ $A/(NkT)$  vs  $x$ ] for case II,  $z = 6$ ,  $r = 2.22$ , and various  $\theta$ 's. Dashed lines (---) show the two conjugate phases. (The metastable regions of the free energy curve have been exaggerated to separate it from the two-phase curve.)

independent of  $r$ , and the central one-phase region remains, as do two very small one-phase regions near  $x = 0$  and  $x = 1$  (see Appendix). Typical free-energy curves that produce this unusual behavior are shown in Figure 5. (Some of the curves are slightly exaggerated to show the effect on the scale shown.)

case III:

$$\epsilon_{ab} = \epsilon_{ay} = \epsilon_{bx} > 0 \rightarrow K_{ab} = K_{ay} = K_{bx} < 1$$

$$\epsilon_{xy} < 0 \rightarrow K_{xy} > 1$$

$$\epsilon_{ax} = \epsilon_{by} = 0 \rightarrow K_{ax} = K_{by} = 1$$

This case (Figure 6) shows qualitatively, for both  $z = 4$  and  $z = 6$ , the same unusual features found for case II with  $z = 6$  (Figures 3–5). As in case II the central one-phase region persists to zero temperature, but, unlike case II, there are no one-phase regions near the pure components (see Appendix). The same low-temperature behavior was found long ago by Barker and Fock<sup>7</sup> for  $z = 6$ , case III (their model II), but they reported only the “critical” (our critical-spinodal) curve and two free-energy curves for  $r = 3$ .

Table 1 shows the coordinates of the special points, the critical double points, and the double critical points. Finally, in Figures 7 and 8 we present the  $\theta$ – $r$  phase diagrams for  $z = 4$  and  $z = 6$  for the three different cases for the sake of comparison. From these, the intermediate character of case II is clear; it is a limiting case of case I because as  $r \rightarrow 0$  they become the same.

## Discussion

The results presented here show that our model, together with the quasi-chemical approximation and extensive computer calculations, can give a rich phase behavior depending on the

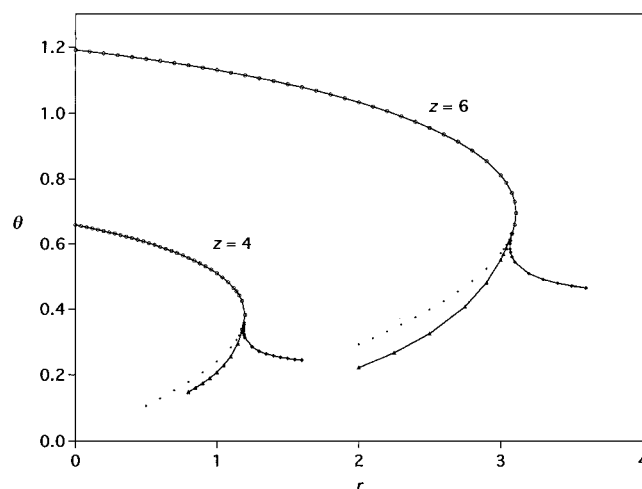


**Figure 6.**  $\theta$ – $r$  master diagrams for case III with  $z = 4$  and  $z = 6$ . Symmetrical critical points,  $\circ$ – $\circ$ ; unsymmetrical critical points,  $\blacklozenge$ – $\blacklozenge$ ; triple points,  $\blacktriangle$ – $\blacktriangle$ ; metastable critical points,  $\bullet$ .

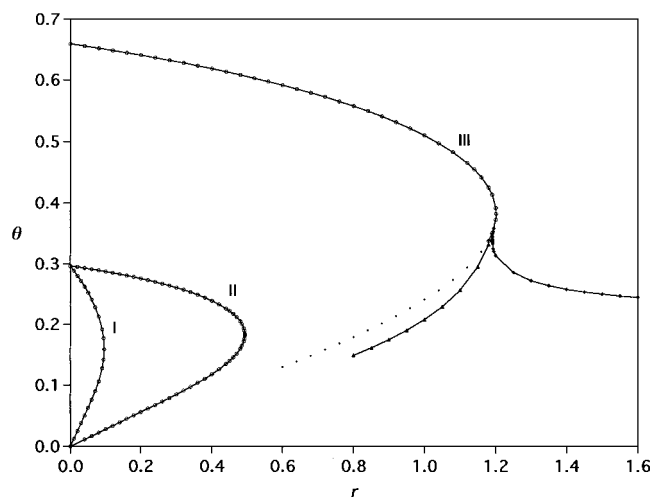


**Figure 7.** Comparison of  $\theta$ – $r$  master diagrams for  $z = 4$ , cases I, II, and III. Symmetrical critical points,  $\circ$ – $\circ$ ; unsymmetrical critical points,  $\blacklozenge$ – $\blacklozenge$ ; triple points,  $\blacktriangle$ – $\blacktriangle$ ; metastable critical points,  $\bullet$ .

**TABLE 1: Special Points**

		critical double points		double critical points	
		$\theta$	$r$	$\theta$	$r$
$z = 4$	case I			0.158 763	0.095 796
	case II			0.1825	0.483 09
	case III	0.3377	1.190 507	0.3819	1.201 04
$z = 6$	case I			0.267 39	0.651 17
	case II	0.308 15	2.214 83	0.469 70	2.382 828
	case III	0.593	3.066	0.695 16	3.109 59

physical considerations set for the interactions between the mixture components.

In case I attractive interactions are stronger than repulsive ones:  $ab$  encounters are repulsive, while the three  $ay$ ,  $bx$ , and  $xy$  are attractive. This combination produces simple closed loops that resemble the type of phase diagram found in hydrogen-bonded systems. However, the closed loops calculated here are necessarily symmetrical because of the symmetry of the interaction energies  $\epsilon$ .

The much larger regions of immiscibility for  $z = 6$  by comparison with those for  $z = 4$  (as shown in Figure 1, and again in Figures 3 and 6) are a direct result of the fact that in our model there are  $(z - 1)^2$  repulsive  $ab$  pairs for every attractive  $xy$  pair. It is worthwhile pointing out that our model predicts loops that are flatter near the lower critical point than

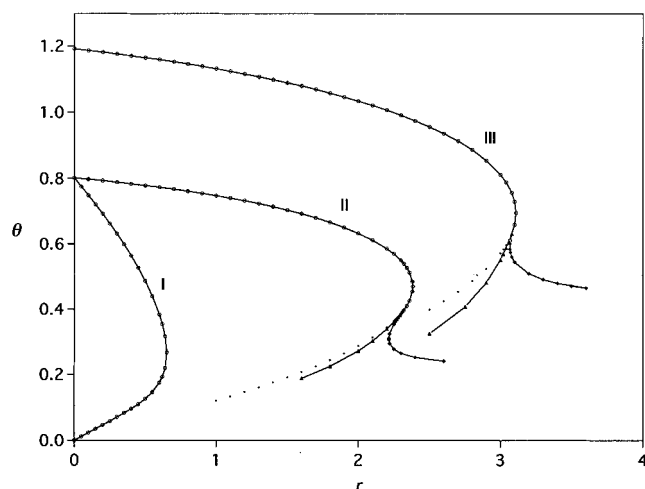


**Figure 8.** Comparison of  $\theta$ - $r$  master diagrams for  $z = 4$ , cases I, II, and III. Symmetrical critical points,  $\circ$ - $\circ$ ; unsymmetrical critical points,  $\blacklozenge$ - $\blacklozenge$ ; triple points,  $\blacktriangle$ - $\blacktriangle$ ; metastable critical points,  $\bullet$ .

near the upper one, a fact that has been observed experimentally;<sup>16</sup> a plot against  $\ln \theta$  might look different.

Case III is a different physical situation, in which the balance between attractive and repulsive interactions produces a richer phase diagram with several two-phase regions and (for one  $r$ ) a critical double point. In this case there is only one attractive interaction  $xy$ , while  $ab$   $ay$ , and  $bx$  are all repulsive.

Our case II calculation shows that this model is indeed intermediate, for  $z = 4$  is very similar to case I and  $z = 6$  is similar to case III. This is the case for mixtures in which there is only one attractive interaction ( $xy$ ) and one repulsive interaction ( $ab$ ), the number of encounters of the last one being larger. With  $z = 6$  the global repulsive interaction is higher (more  $ab$  pairs) so that the phase behavior is similar to case III, while for  $z = 4$  they are not able to overcome the attractive interactions, so the phase diagrams are similar to case I.

Although, to the best of our knowledge, experimental examples of the complex phase diagrams we have found are not yet known, it is surprising that it is only case I that consistently yields simple closed-loop diagrams. It seems to us that case I is physically unreasonable since it assumes that  $a$  interacts with  $y$  (and  $b$  with  $x$ ) with the same strong attraction as  $x$  with  $y$ . The assumptions of case II (or even case III) seem more plausible.

Barker and Fock<sup>7</sup> used the quasi-chemical approach with a model substantially the same as ours.<sup>17</sup> The results for their "model I" (our case I) for  $z = 4$  and  $z = 6$  are essentially identical with ours. They reported for their "model II" (our case III) a single free-energy curve showing the separate two-phase regions that we have explored in detail. Apparently they did not pursue these phase diagrams because none were known experimentally.

The papers using decorated lattices,<sup>9</sup> renormalization group theory,<sup>10</sup> and simulation methods<sup>11</sup> all obtained closed loops, but their main concern was to widen the coexistence region to get better agreement with experimental systems. Extra features such as the ones we found were not reported.

Corrales and Wheeler<sup>12</sup> examined phase equilibria in chemically reacting ternary systems both with a mean-field model and with a decorated lattice model. They found, with both models, not only closed loops similar to those found in hydrogen-bonded systems, but also some low-temperature unsymmetrical two-phase regions similar to our case III results.

Jackson<sup>13</sup> calculated the phase equilibria of binary mixtures with mean-field attractive forces between like species and none

between unlike molecules, using an "augmented" van der Waals equation of state, and in which phase diagrams depend on an association parameter that mimics our orientational interaction between molecules. He reported that for a low value of the association parameter only a symmetrical two-phase region is observed, while for a higher value there is a triple point above two separate two-phase coexistence regions, and only for a very strong value of the association parameter are there closed loops.

More recently, Talanquer<sup>14</sup> reported extensive results for a ternary regular solution model in which an addition reaction of the type  $X + Y = Z$  takes place. In this work, the Gibbs free energy and the entropy of the chemical reaction are the main parameters that determine the difference between this mixture and one without a chemical reaction taking place. In some of his examples there are, in addition to closed loops, triple points, unsymmetrical critical points, and other features that we have found in our case III.

That the phase diagrams determined in these last three studies are similar to ours is not surprising since the physics of all four is similar. The form of our phase diagrams depends upon the magnitude of the attractive constant  $\epsilon_{xy}$ , which we translated into a constant  $K_{ab}$ ; these are roughly equivalent to Jackson's association parameter<sup>12</sup> or to the chemical equilibrium constants of Corrales and Wheeler<sup>13</sup> and of Talanquer.<sup>14</sup> However, none of these other models yielded a nonzero central one-phase region in the limit of zero temperature; this difference we attribute (Appendix) to the fact that all of these models involve assumptions that are equivalent to setting  $z = \infty$ . In the Appendix we will consider whether this Barker-Fock model is physically reasonable in the limit of very low temperatures.

We see that this quasi-chemical model, although partially explored many years ago, has a wealth of interesting features not previously recognized and yields phase diagrams that, while differing in detail, can be related to those obtained from other models and approximations.

## Appendix

**Phase Separation as  $T \rightarrow 0$ .** Before considering whether the Barker-Fock model is physically reasonable at low temperatures, we first outline the mathematical results of carrying the model to the limit of zero temperature.

For case III it is easy to obtain an explicit result for the limiting phase separation as the temperature approaches zero. In this case  $K_{ab} = K_{ay} = K_{bx} \rightarrow 0$ , while  $K_{xy} \rightarrow \infty$ . We must destroy the symmetry of the conservation equations by imposing the condition that  $x > 1/2$ . In this case there are more  $b$ 's than  $a$ 's and more  $y$ 's than  $x$ 's. It follows because of the large size of  $K_{xy}$  that virtually all the  $x$ 's are bound to  $y$ , so there are substantially no  $a$ - $x$  pairs. Equations 6 then simplify to

$$(1 + \xi_{aa})^{1/2}(1 - x)(z - 1)(1 + \xi_{aa})^{1/2} = z$$

$$(1 + \xi_{xx})^{1/2}xK_{xy}^{1/2}(1 + \xi_{yy})^{1/2} = z$$

$$(1 + \xi_{bb})^{1/2}x[(z - 1)(1 + \xi_{bb})^{1/2} + (1 + \xi_{yy})^{1/2}] = z$$

$$(1 + \xi_{yy})^{1/2}\{(1 - x)K_{xy}^{1/2}(1 + \xi_{xx})^{1/2} + x[(z - 1)(1 + \xi_{bb})^{1/2} + (1 + \xi_{yy})^{1/2}]\} = z \quad (\text{A.1})$$

If we substitute from the second equation into the fourth, we obtain a simpler equation:

$$(1 + \xi_{yy})^{1/2} x [(z - 1)(1 + \xi_{bb})^{1/2} + (1 + \xi_{yy})^{1/2}]^{1/2} = z(2x - 1)/x$$

Solving these equations we obtain for each of the deviation functions:

$$\begin{aligned} 1 + \xi_{aa} &= \frac{z}{(z - 1)(1 - x)} \\ 1 + \xi_{xx} &= \frac{z[(z + 1)x - 1]}{K_{xy}(2x - 1)^2} \\ 1 + \xi_{bb} &= \frac{z}{(z + 1)x - 1} \\ 1 + \xi_{yy} &= \frac{(2x - 1)^2 z}{x^2 [(z + 1)x - 1]} \end{aligned} \quad (\text{A.2})$$

These can now be substituted into eq 4 to obtain an explicit equation for the free energy. (One must not forget that there are  $(z - 1)$   $a$ 's and  $(z - 1)$   $b$ 's.)

$$\begin{aligned} \frac{\Delta A}{NkT} &= -\frac{(1 - x)}{2} \ln K_{xy} + \left(\frac{z}{2}\right) \ln z + (2x - 1) \ln(2x - 1) - \\ &\frac{(1 - x)(z - 1)}{2} \ln(z - 1) - \frac{(1 - x)(z - 3)}{2} \ln(1 - x) - \\ &\frac{[(z + 1)x - 1]}{2} \ln[(z + 1)x - 1] \end{aligned} \quad (\text{A.3})$$

The first term on the right is  $\Delta H/NkT$ , which would be  $-\infty$  if  $K_{xy}$  were infinite. For a very large but finite  $K_{xy}$  this produces a  $\Delta H$  that consists essentially of two straight lines starting at zero at  $x = 0$  and  $x = 1$  and intersecting at a very large negative number at  $x = 1/2$ . Since phase equilibrium depends upon finding a straight line tangent to a reentrant curve, this term contributes nothing to the solution of the problem; the remaining terms constitute  $-\Delta S/Nk$ . First-order corrections to eq A.3 for finite  $K_{xy}$  are proportional to  $\exp(-\beta\epsilon)$ , which goes to zero faster than the limiting  $T\Delta S$  terms.

Now one must get the coexistence limits from eq A.3 by bringing up a tangent straight line to the free energy curve (or more accurately the entropy curve). One suspects (and this can be confirmed by plotting the curve) that one coexistence limit is at  $x = 1$  (where the line does not have to be tangent). If so, one simply finds the tangent line that goes through 0 at  $x = 1$ . In other words, one must solve the equation

$$\Delta S + (1 - x)(\partial \Delta S / \partial x) = 0 \quad (\text{A.4})$$

There is considerable cancellation in terms, and one ends up with

$$\frac{z}{2} \ln \left[ \frac{(z + 1)x - 1}{z} \right] - \ln(2x - 1) = 0 \quad (\text{A.5})$$

First, we note that  $x = 1$  is a solution for all  $z$ . (This should come as no surprise; we put that feature into eq A.4.) For  $z = 2$ , that is the only solution.

For all values of  $z$  greater than 2 (including noninteger values) there are two roots to eq A.5, one at  $x = 1$ , and a second somewhere between  $x = 0.5$  and  $+\infty$ . For  $z = 3$ , there are two roots, both at  $x = 1$ . We conclude that, for  $z = 3$ , there is complete miscibility at  $T = 0$ .

For all  $z$ 's between 3 and infinity, the second root lies between 0.5 and 1.0, so there is a miscibility gap. For  $z = 4$ , the second root is at  $x = 17/25 = 0.68$ . Thus, there is a miscibility gap between 0.68 and 1.00 (and, of course, between 0.00 and 0.32). Between 0.32 and 0.68 there is complete miscibility at  $T = 0$ . For  $z = 6$ , eq A.5 yields a much smaller miscibility region, between  $x = 0.4440$  and 0.5560. For  $z = 12$ , the range is still smaller, only between  $x = 0.4950$  and 0.5050.

For  $z = \infty$ , the left-hand term in eq A.5 is zero, so  $x$  is exactly  $1/2$ . Thus the reason that Corrales and Wheeler,<sup>12</sup> Jackson,<sup>13</sup> and Talanquer<sup>14</sup> all found coexistence curves that went to  $x = 1/2$  as  $T \rightarrow 0$  is presumably that their models are all equivalent to an assumption that  $z = \infty$ .

The situation for case II is more complicated and leads to surprising results. The conservation conditions equivalent to eq A.1 contain additional terms because pairs  $ay$  and  $bx$  are now allowed. The resulting expressions for the deviation parameters are quadratic and have to be solved numerically. For  $z = 6$  the central one-phase region extends from  $x = 0.32478$  to  $x = 0.67522$ . However, unlike case III, there are small one-phase regions near the pure components. These regions, which extend from  $x = 0$  to  $x = 0.00532$  and from  $x = 0.99468$  to  $x = 1$ , are too small to be seen in the phase diagrams of Figure 4. Presumably they occur because  $bx$  pairs are significant near  $x = 0$ , while  $ay$  pairs are significant near  $x = 1$ .

Finally, we consider the physical reasonableness of this unusual limiting behavior. There are several potential problems:

1. The quasi-chemical model assumes a quasi-lattice and is thus incapable of distinguishing between fluids and solids. At low temperatures the system is surely crystalline, and the third law of thermodynamics requires that if the system is truly in internal equilibrium it must, as  $T \rightarrow 0$ , separate into ordered structures, that is, A, B, and AB with the  $x$  and  $y$  faces part of a completely ordered array. If there are any one-phase fluid regions of variable composition; they must be metastable glasses.

2. An examination of eq A.3, in which all the terms on the right-hand side (except the first which is  $\Delta H/NkT$ ) constitute  $-\Delta S/Nk$ , shows that  $\Delta S$  is negative for all values of  $x$  (except of course 0 and 1). Indeed the most negative value of  $\Delta S$  is that for  $x = 1/2$ . This would seem to violate the third law. However, the assumption that  $K_{ax} = K_{by} = 1$  (which cannot be exactly true) leaves the pure components completely disordered; thus, a negative entropy produced by the  $x$ - $y$  ordering is not unreasonable. The complete ordering of the system to remove any one-phase region of variable composition is not part of the present Barker-Fock model (although it could be added by adjusting  $K_{ax}$  and  $K_{by}$ ) and would actually occur only at very small values of  $\theta$ , perhaps too small to show on our figures.

3. Walker and Vause<sup>10</sup> have noted that the Barker-Fock model shows "frustration" in that it is impossible for all bonds (pairs?) to achieve simultaneously their most favorable energies as  $T \rightarrow 0$ . (This does not seem to apply to the ordered structure at  $x = 1/2$ .) This suggests that Barker-Fock critical behavior is not Ising-like and that the details of phase transitions will be wrong. It is well-known that this model (indeed the quasi-chemical method in general) does not yield the proper width of coexistence curves or nonclassical behavior at critical points (thus our critical double points have the wrong exponents), but we doubt that this deficiency invalidates our qualitative results. We believe that the fact that Corrales and Wheeler,<sup>12</sup> Jackson,<sup>13</sup> and Talanquer<sup>14</sup> (whose models are presumably free of frustration) all got two separate coexistence regions as  $T \rightarrow 0$  at least partially validates our model and that the nonzero one-phase regions we found can reasonably be attributed to the finite  $z$ 's.

## References and Notes

- (1) Munster, A. *Trans. Faraday Soc.* **1950**, 46, 165.
- (2) Barker, J. A. *J. Chem. Phys.* **1952**, 20, 1526.
- (3) Tompa, H. *J. Chem. Phys.* **1953**, 21, 250.
- (4) Guggenheim, E. A. *Proc. R. Soc.* **1935**, A148, 304.
- (5) Rowlinson, J. S.; Sutton, J. R. *Proc. R. Soc.* **1955**, A229, 271.
- (6) Balescu, R. *Bull. Acad. Belg. Cl. Sci.* **1955**, 41, 1242.
- (7) Barker, J. A.; Fock, W. *Discuss. Faraday Soc.* **1953**, 15, 188.
- (8) Wheeler, J. C. *Annu. Rev. Phys. Chem.* **1977**, 28, 411.
- (9) Anderson, G. R.; Wheeler, J. C. *J. Chem. Phys.* **1978**, 69, 2082.
- (10) Walker, J. S.; Vause, C. A. *J. Chem. Phys.* **1983**, 79, 2660.
- (11) Gubbins, K. *Mol. Simul.* **1989**, 2, 223.
- (12) Corrales, L. R.; Wheeler, J. C. *J. Chem. Phys.* **1989**, 91, 7097.
- (13) Jackson, G. *Mol. Phys.* **1991**, 72, 1365.
- (14) Talanquer, V. *J. Chem. Phys.* **1992**, 96, 5408.
- (15) The formulation of the quasi-chemical equations in terms of the deviation parameter  $\xi$  is derived from an unpublished paper by one of us (R.L.S.) whose purpose was to show that the leading terms in the free energy resulting from series expansions of  $\ln(1 + \xi)$  are quadratic, not linear, in the  $\xi$ 's. There is no special virtue to this formulation in the context of this paper.
- (16) Francis, A. W. *Liquid-liquid Equilibrium*; John Wiley: New York, 1963.
- (17) The coordinates in the Barker and Fock figures differ from ours. Their abscissa  $m$  is our  $r$ , but their ordinate  $kT/U_I$  differs from our  $\theta = kT/(2\epsilon_{ab})$  by a factor  $2 \times 2.303$ .